TELECOMMUNICATIONS AND RADIO ENGINEERING

b begell

New York • Connecticut

TELECOMMUNICATIONS AND RADIO ENGINEERING

CONTENTS

APPLIED RADIO PHYSICS: SPACE, ATMOSPHERE, AND EARTH'S SURFACE RESEARCH

EMPIRICAL MODEL OF THE MIDDLE LATITUDES LOWER IONOSPHERE FOR MODELING OF HF AND VHF RADIO WAVES PROPAGATING

A.M. Gokov,[1,♦] O.F. Tyrnov,[2] & Yu.V. Buts[1]

[1]S. Kuznets Kharkiv National University of Economics, Ministry of Education and Science of Ukraine, 9A Nauka Ave., Kharkiv 61166, Ukraine

[2]V. Karazin Kharkiv National University, 4 Svobody Sq., Kharkiv 61022, Ukraine

♦Address all correspondence to: A.M. Gokov, E-mail: 19amg55@gmail.com

On the basis of the experimental electron density profiles N(z) obtained under quiet conditions at the V.N. Karazin Kharkiv National University by partial reflection technique, there were constructed average-daily seasonal <N(z)> and their height gradients d<N>/dz profiles which were used for model calculating characteristics of the radio waves scattered by turbulent N irregularities.

KEY WORDS: *electron density, mid-latitude D-region of the ionosphere, model of region D, partial reflection method.*

1. INTRODUCTION

In order to predict characteristics of radio waves scattered by turbulent irregularities of the electron density, *N*, determining of kinds of three-dimension spectrum function fluctuations, $F_N(\vec{p})$, ($\vec{p}$ - being the wave vector) is the most important aspect. Expressions for $F_N(\vec{p})$ are known elsewhere [1]. Spectrum changes in space and time are very important for practical using formulas in order to obtain characteristics of the ionosphere and signals scattered by turbulent irregularities. The measure variability of electron density irregularities, g_N, caused by vertical gradient of the averaged *<N(z)>* profile (*z* being the height above the Earth surface) makes the largest contribution to space-time $F_N(\vec{p})$ changes. Note that the g_N variability caused by turbulent exchange

coefficient has been studied rather well [2]. Therefore, it is necessary to have a mode of $<N(z)>$ suitable l for solving this problem. At present, a number of $<N(z)>$ models are known [2–13]. Among them, only models of [4–7]) are based on the similar data obtained by the same method in the same place. (Data obtained by different methods in various places of the Earth lead to ineradicable and unknown errors in modeling). Besides, these models have no sufficient statistical reliability for different conditions (time of year and day, effects of natural disturbances, etc.).

Our paper presents a model of average-daily seasonal $<N(z)>$ profiles of the middle latitude (ML) D-region of the ionosphere from measurements by the partial reflection (PR) technique obtained near Kharkiv. For each of the conditions, the $N(z)$ statistics are several times larger than the number of the data in [2–13]. On the basis of a turbulent nature of scattering irregularities and the $<N(z)>$ model developed, a numerical modeling of characteristics of HF and VHF radio waves propagating obliquely was carried out.

2. EXPERIMENTAL EQUIPMENT AND INVESTIGATION METHODS

Our investigations were carried out on the basis of a retrospective analysis of the data obtained by the partial reflection technique over 1972 to 2018. The measurements of partially-reflected signals and radio noise were conducted using the equipment from [14] in the middle latitude in the vicinity of Kharkiv (geographic coordinates $\varphi =49.5°$N, $\lambda = 36.3°$E).

The main parameters of the facility are as follows: the operating frequencies being $f = 2$-4 MHz, the duration of sounding pulses being 25 mcs with the repetition frequency $F = 1$–5 Hz. The amplitudes, $A_{no,x}$, of radio noise and those of mixture of radio noise and partially-reflected signals, $A_{o,x}$, of the ordinary (o) and extraordinary (x) magnetic-ionic components were recorded at 15 height levels (beginning from 45 or 60 km) in a 3-km step. The measurements of $A_{no,x}(t)$ and $A_{o,x}(z,t)$ (here t is the time) were made over 1972-2018 for different seasons both for the fixed zenith solar angles ($\chi = 60°$, $75°$, $78°$) over several month of a year and for the diurnal cycles (continuously or in 30 - 90 min). The duration of the records selected for obtaining $N(z)$ was 10 min.

To construct a model of electron concentration profiles in the mid-latitude lower ionosphere, 4.600 $<N(z)>$ profiles with an evenly distributed over the seasons were used [15]. The data were obtained under undisturbed conditions only using the PR method. To obtain $<N(z)>$ profiles two or more methods were simultaneously applied [16,17], which is necessary and made it possible to minimize the errors in determining the parameters of the lower ionosphere.

Relative to the daily (day) changes for each season, the same in the number of arrays of measurements $<N(z)>$ were used with an approximately uniform distribution in the daytime. The error of the $N(z)$ calculations over the whole height range was ≤ 30 %.

3. A MODEL OF AVERAGE-DAILY SEASONAL PROFILES OF THE ELECTRON DENSITY

In order to construct models of average-daily seasonal electron density profiles $\langle N(z) \rangle$, there were used 4600 $N(z)$ profiles having rectangular distributions in the seasons (which is one of the important distinctions from the models presented in [2-13]). At the same time, there were used the $N(z)$ profiles obtained under quiet conditions (i.e., when there were neither artificial or natural disturbances such as solar flares, powerful earthquakes, thunderstorms, solar terminator, etc.).

As to the diurnal (day-time) variation, there were used the similar as to their number for each season day-time $N(z)$ measurements with their approximately rectangular distribution for light time of the day. That allowed to obtain seasonal average-daily $\langle N(z) \rangle$ profiles and - on the basis the N scattering for each concrete height – make an estimation of the contribution to the deviation of N from the average value of various physical processes.

The seasonal average-daily $\langle N(z) \rangle$ profiles were obtained by means of calculating median values of $\langle N \rangle$ over the heights interval of $z = 70 - 95$ km with a step of $\Delta z = 2.5$ km. The calculation results are presented in Table 1 (in brackets in the first column there are given the numbers of N values used while counting $\langle N \rangle$).

TABLE 1: The seasonal average-daily $\langle N(z) \rangle$ profiles

z, km	$\langle N \rangle \cdot 10^{-2}$, cm^{-3}			
	Winter	Spring	Summer	Autumn
70.0 (640)	2.0	1.0	2.8	0.9
72.5 (710)	3.0	3.1	3.0	3.0
75.0 (2400)	5.0	4.4	3.5	5.0
77.5 (3100)	7.5	7.3	4.5	6.1
80.0 (3800)	10.0	8.5	6.2	7.2
82.5 (3400)	16.0	10.0	8.2	11.0
85.0 (3750)	22.8	15.1	14.0	17.3
87.5 (3600)	35.8	19.7	21.0	25.4
90.0 (2450)	41.0	26.0	32.0	41.0
92.5 (2500)	51.0	36.0	41.0	50.2
95.0 (1800)	54.0	42.0	47.0	53.0

Vertical gradients of $\langle N(z) \rangle$ may be estimated from the Table 1 data using the following relationship:

$$\Delta < N > / \Delta z = \left(< N > \left(z_{i+1} \right) - < N > \left(z_i \right) \right) / 2.5 \cdot 10^5,$$

here $\Delta z = z_{i+1} - z_i$, $i = 1, 2, ..., 11$, and $i = 1$ corresponds to $z = 70$ km.

Their calculation results are given in Table 2.

TABLE 2: Vertical gradients of the seasonal average-daily $< N(z) >$ profiles

z, km	$(\Delta <N>/ \Delta z) \cdot 10^3$, cm^{-4}			
	Winter	Spring	Summer	Autumn
70 - 72.5	0.4	0.8	0.1	0.8
72.5 - 75	0.8	0.5	0.2	0.8
75 - 77.5	1.0	1.2	0.4	0.5
77.5 - 80	1.0	0.5	0.7	0.5
80 - 82.5	2.4	0.6	0.7	1.5
82.5 - 85	2.8	1.6	1.2	2.4
85 - 87.5	4.8	2.0	3.6	3.2
87.5 - 90	2.4	2.4	4.8	6.4
90 - 92.5	3.6	4.0	3.6	3.6
92.5 - 95	1.6	2.8	2.4	1.2

It is known that the N value at any moment of time may be expressed as:

$$N = <N>\pm N^*,$$

where N^* is the deviation from the average value $<N>$, caused by the different physical processes and measurement errors.

The main causes of $N(z)$ variability in the D-region of the ionosphere are as follows: diurnal and seasonal ionization changes, cyclic solar-activity changes, meteorological processes and hydrodynamic turbulence.

To a certain extent, these N-variability changes may be considered independent, and then for a resulting N-dispersion at the fixed height the following relation is valid:

$$\sigma_N^2(1\pm\Delta_N) = \sigma_1^2(1\pm\Delta_1) + \sigma_2^2(1\pm\Delta_2) + \sigma_3^2(1\pm\Delta_3) + \sigma_4^2(1\pm\Delta_4) + \sigma_5^2(1\pm\Delta_5), \quad (1)$$

where indices 1–5 correspond to the components caused by the turbulence, meteorological processes, diurnal and seasonal variations, solar activity changes respectively, $\Delta_k = D_k / \sigma^2$, D_k – being their dispersions of the errors, $k = 1, 2, …, 5$.

Let as determine a contribution of the processes mentioned above to the total N-variability.

The calculation results are given in Tables 3 and 4. Table 3 contains estimations of the contributions of individual components of the intra seasonal variability of the value of N for individual heights intervals Δz; both contributions and their root mean square deviations are given in per cent.

Table 4 contains the contributions of various physical mechanisms to the variability of N in the D-region for different heights intervals Δz and seasons.

For comparison, we calculated $<N>$ and the contribution of various physical mechanisms to the variability of N in the D-region of the ionosphere for data catalogs of profiles $N(z)$ of the mid-latitude lower ionosphere for different regions of the planet. The calculation results for the summer are given in Tables 5–7 for: a catalog [7] for a part of the Siberian region of Russia, a NIRFI catalog [4] (data obtained by the PR method) and a data bank of $N(z)$ measurements using an electrostatic probe on an MR-100B rocket (missile launches were carried out near the Volgograd city) [11].

TABLE 3: The contributions of individual components of the intra seasonal variability of the value of N for individual heights intervals

Season	Δz = 70–82.5 km				Δz = 82.5–95 km			
	σ_1^2, %	σ_2^2, %	σ_3^2, %	σ_5^2, %	σ_1^2, %	σ_2^2, %	σ_3^2, %	σ_5^2, %
Winter	3.5 ± 0.8	75.1 ± 4.5	21.2 ± 3.2	2.1 ± 1.1	3.4 ± 1.1	71.0 ± 9.0	25.1 ± 5.0	0.6 ± 0.3
Spring	4.3 ± 0.9	72.0 ± 6.0	21.5 ± 4.0	2.2 ± 0.9	7.1 ± 1.3	65.0 ± 8.0	27.9 ± 4.7	1.1 ± 0.9
Summer	4.8 ± 1.1	70.2 ± 4.1	22.8 ± 3.7	2.6 ± 1.3	6.5 ± 1.0	63.2 ± 8.7	29.2 ± 6.0	1.1 ± 0.7
Autumn	6.8 ± 1.0	71.0 ± 5.7	21.2 ± 4.1	2.5 ± 1.1	6.6 ± 0.7	64.8 ± 8.2	28.4 ± 3.8	1.0 ± 0.6

TABLE 4: The contributions of various physical mechanisms to the variability of N

	Δz, km	70-72.5	72.5-75	75-77.5	77.5-80	80-82.5	82.5-85	85-87.5	87.5-90	90-92.5	92.5-95
$(\sigma_N)^2$· 10^4, cm^{-3}	Winter	0.6 ±0.2	1.1±0.3	1.8±0.4	5.3±0.8	6.4±1.1	14.0±3.6	32.0±7.1	68.0±15	62.0±14	66.0±15
	Spring	0.4 ±0.2	1.0±0.3	1.5±0.3	4.4±0.7	6.2±1.0	14.0±4.1	28.0±6.2	59.0±14	50.0±12	59.0±15
	Summer	0.4 ±0.2	0.9±0.3	1.8±0.4	4.8±0.9	5.4±1.1	12.0±3.3	26.0±5.9	57.0±13	51.0±12	56.8±13
	Autumn	0.8±0.3	0.8±0.3	1.7±0.5	4.9±0.9	6.2±1.0	14.6±3.7	37.0±7.4	64.0±16	56.0±13	62.0±14
$(\sigma_1)^2$· 10^{-5}, cm^{-3}	Winter	0.5±0.2	0.9±0.3	0.8±0.3	1.2±0.3	2.9±0.6	8.6±1.9	11.0±3.1	17.9±4.9	16.8±4.0	15.0±4.1
	Spring	0.1±0.03	0.7±0.2	0.6±0.2	1.3±0.4	1.7±0.5	10.4±3.3	28.0±6.2	26.0±6.2	22.0±5.4	23.2±5.5
	Summer	0.1±0.04	0.6±0.2	0.8±0.3	1.2±0.4	2.8±0.6	8.4±1.4	29.0±6.0	16.2±4.9	16.3±4.4	16.3±3.8
	Autumn	0.2±0.06	0.8±0.3	1.3±0.3	1.3±0.3	2.5±0.6	14.4±3.8	19.5±5.0	25.4±6.1	18.9±4.1	19.9±4.2
$(\sigma_2)^2$· 10^4, cm^{-3}	Winter	0.4±0.2	0.8±0.3	1.4±0.5	3.8±1.1	4.1±1.6	10.6±2.8	22.8±8.6	40.0±12	38.0±11	38.0±12
	Spring	0.3±0.1	0.5±0.2	0.8±0.3	3.2±1.0	3.2±0.9	8.0±2.4	18±5.0	36±9.6	31±5.7	37±10
	Summer	0.3±0.1	0.6±0.2	1.1±0.4	2.8±0.5	2.6±0.5	7.5±2.8	16.0±4.8	36.0±8.9	33.0±8.1	35.9±9.0
	Autumn	0.6±0.2	0.4±0.2	1.9±0.5	3.3±1.1	3.8±1.4	9.6±3.0	25.0±7.8	37.2±11	37.1±10	38.1±10
$(\sigma_3)^2$· 10^4, cm^{-3}	Winter	0.1±0.04	0.2±0.06	0.3±0.1	1.3±0.3	1.9±0.7	2.4±0.75	7.9±2.4	18.0±4.9	20.0 ±4.9	16.0 ±4.8
	Spring	0.1±0.04	0.3±0.1	0.5±0.1	1.1±0.4	2.7±0.9	3.8±1.1	6.9±2.1	20.0±5.0	18.0±4.2	19.0±4.8
	Summer	0.1±0.04	0.3±0.15	0.4±0.11	1.8±0.65	1.9±0.7	3.5±1.2	6.8±2.3	19.0±5.1	17.3±4.7	18.8±5.1
	Autumn	0.2±0.1	0.3±0.1	0.2±0.1	1.2±0.4	2.1±0.7	4.4±1.3	9.6±1.8	21.0±6.3	19.4±6.4	20.2±6.3
$(\sigma_5)^2$· 10^{-6}, cm^{-3}	Winter	4.0±1.3	3.5±1.3	3.0±0.8	8.0±2.4	11.0±2.9	14.0±4.0	20.0±4.7	21.0±5.8	20.0±5.3	21.4±5.3
	Spring	1.0±0.3	2.5±0.8	3.0±0.8	7.0±2.1	8.0±2.4	16.0±4.8	36.0±8.7	40.0±9.9	40.0±8.4	38.2±7.7
	Summer	1.2±0.4	1.0±0.3	4.0±0.9	8.1±2.6	12.0±3.1	16.0±3.7	30.2±7.6	38.0±9.1	31.0±7.7	36.2±7.6
	Autumn	1.5±0.5	2.0±0.6	6.0±1.1	7.1±2.1	10.0±3.3	14.0±4.8	25.0±5.9	46.0±14	44.0±17	44.0±16

TABLE 5: Calculations of the contribution of the components of variability N for summer according to the catalog [7]

$z,$ km	$<N> \cdot 10^{-2}$ cm^{-3}	$\triangle z,$ km	$\sigma_N^2 \cdot 10^{-4},\ \%$	$\sigma_5^2 \cdot 10^{-2},\ \%$	$\sigma_1^2 \cdot 10^{-2}, \%$	$\sigma_3^2 \cdot 10^{-4},$ $\%$	$\sigma_2^2 \cdot 10^{-4}, \%$
70.0	2.7	72.5-70.0	0.11±0.05	0.21±0.02	0.27±0.11	0.044±0.01	0.09±0.02
72.5	3.3	75.0-72.5	0.41±0.11	0.32±0.09	0.36±0.11	0.049±0.01	0.31±0.09
75.0	4.1	77.5-75.0	1.28±0.31	0.71±0.12	1.14±0.31	0.288±0.04	0.88±0.22
77.5	6.4	80.0-77.5	3.52±0.91	1.3±0.18	1.10±0.21	1.250±0.27	2.45±0.61
80.0	9.1	82.5-80.0	4.51±1.40	0.91±0.19	2.20±0.44	1.610±0.31	3.31±0.52
82.5	11.2	85.0-82.5	9.14±2.68	1.54±0.26	6.61±0.77	2.640±0.49	6.97±1.85
85.0	19.4	87.5-85.0	22.00±4.8	1.34±0.31	9.91±1.81	6.660±1.27	17.10±2.5
87.5	27.0	90.0-87.5	41.11±7.9	1.92±0.29	25.1±4.83	13.97±2.38	25.40±4.9
90.0	36.0						

TABLE 6: Calculations of the contribution of the components of variability N for summer according to the catalog [11]

$z,$ km	$<N> \cdot 10^{-2},$ cm^{-3}	$\triangle z,$ km	$\sigma_N^2 \cdot 10^{-4},$ $\%$	$\sigma_5^2 \cdot 10^{-2},$ $\%$	$\sigma_1^2 \cdot 10^{-2},$ $\%$	$\sigma_3^2 \cdot 10^{-4},$ $\%$	$\sigma_2^2 \cdot 10^{-4},$ $\%$
72.5	3.3	75.0-72.5	0.47±0.13	0.3±0.08	0.35±0.1	0.045±0.01	0.36±0.08
75.0	4.1	77.5-75.0	1.20±0.30	0.7±0.11	1.10±0.3	0.240±0.04	0.78±0.20
77.5	5.9	80.0-77.5	3.70±1.00	1.0±0.18	1.0±0.2	1.150±0.21	2.35±0.51
80.0	9.6	82.5-80.0	4.5±1.10	0.9±0.18	2.10±0.4	1.400±0.31	2.80±0.51
82.5	13.5						

TABLE 7: Calculations of the contribution of the components of variability N for summer according to the catalog [4]

$z,$ km	$<N> \cdot 10^{-2}$ cm^{-3}	$\triangle z,$ km	$\sigma_N^2 \cdot 10^{-4},$ $\%$	$\sigma_5^2 \cdot 10^{-2},$ $\%$	$\sigma_1^2 \cdot 10^{-2},$ $\%$	$\sigma_3^2 \cdot 10^{-4},$ $\%$	$\sigma_2^2 \cdot 10^{-4},$ $\%$
70.0	3.7	72.5-70.0	0.18±0.05	0.21±0.03	0.26±0.11	0.033±0.01	0.07±0.02
72.5	3.9	75.0-72.5	0.48±0.11	0.34±0.08	0.36±0.11	0.041±0.01	0.38±0.08
75.0	4.4	77.5-75.0	1.27±0.34	0.78±0.13	1.17±0.31	0.198±0.04	0.81±0.20
77.5	5.9	80.0-77.5	3.77±1.11	1.13±0.19	1.22±0.22	1.200±0.22	2.45±0.48
80.0	9.8	82.5-80.0	4.57±1.19	0.89±0.18	2.08±0.42	1.410±0.30	2.71±0.48
82.5	13.8	85.0-82.5	10.71±3.0	1.58±0.27	6.66±0.71	2.400±0.49	7.55±1.44
85.0	19.2	87.5-85.0	22.22±5.11	1.41±0.31	9.66±1.32	6.660±1.28	16.44±2.5
87.5	31.0	90.0-87.5	42.23±8.05	2.10±0.28	22.1±4.62	13.98±2.41	24.40±4.2
90.0	38.0						

A comparison of the given <N> and the contribution of various physical mechanisms to the variability of the electron concentration in the D-region of the ionosphere for these catalogs of profiles $N(z)$ of the mid-latitude lower ionosphere of different regions of the planet shows their good agreement. On the other hand, the values of seasonal daily average <$N(z)$> profiles differ markedly, due to both the heterogeneity and limitedness of the data banks used and the regional features of the lower ionosphere.

Thus, it has been established from the data presented that the main contribution to the total variability of the altitude profiles $N(z)$ in the mid-latitude D-region under non-disturbed conditions is made by meteorological processes and diurnal ionization variability.

We also note that the considered regional model can be used to solve practical problems, for example, to solve the problems of radio navigation, predicting the propagation of radio waves in near-Earth space [16].

4. MODELING OF RADIO WAVE CHARACTERISTICS

Let as consider some characteristics of radio waves scattered by turbulent irregularities of N in the D-region of the ionosphere. In order to do this, we shell use a model of $\langle N(z) \rangle$ profiles and their variability in space and time on the basis of the data given above. We shall consider a path of the oblique propagation of radio waves (a transmitter and a receiver are spaced apart) as a propagation model. A particular case here is investigating of back scattering when the transmitter and receiver are located in the same place. The frequencies of the radio waves used being $f = 5$–100 MHz.

The theory of radio wave propagation knows an expression allowing to calculate a quantity of the scattered power, P_s, at the input of a receiving device if characteristics of the path, operating frequency, and spectrum density of the electron concentration fluctuations, F_N, are known [1]:

$$\frac{P_s}{P_o} = \left(\frac{80.8}{c^2} \right)^2 \frac{\pi^3 \lambda^2}{2} \int_V \frac{F_N F_1^2 F_2^2}{R_1^2 \cdot R_2^2} sin^2 \alpha_1 \cdot dV , \qquad (2)$$

here P_0 is the energy transmitted by an undirected antenna, F_1 and F_2 are the field antenna diagrams of the receiving and transmitting antennas, R_1 and R_2 are the distances of the elementary dV of the scattering volume, V, up to points of transmitting and receiving, α_1 is the angle between the polarization direction of a incident wave on the elementary volume, dV, of the wave and the direction from its center to the receiving point.

At first, consider a case of vertical sounding. For the calculations there were taken the following parameters of a receiving-transmitting system: $P_0 = 60$ kW, the width of the main lobe at the half-power is $\theta_0 = 5°$, the amplification coefficient of an antenna, $G = 100$. For different values of $\langle N(z) \rangle$ from Table 1 and $f = 30$ and 100 MHz, there were calculated P_s values, i.e., sensitivity thresholds of the receivers were determined. The P_s values at $f = 30$ MHz for different $\langle N(z) \rangle$ and $d\langle N \rangle/dz$ values from Tables 1 and 2 appeared to be $P_s \sim 10^{-12} - 10^{-13}$ W, for $f = 100$ MHz, $P_s \sim 10^{-13} - 10^{-14}$ W.

In the case of oblique propagation, characteristics of receiving-transmitting antennas were set equal: the width, θ_0, of the direction diagram at the half-power in a

horizontal plane, being $\theta_0 = 5^o$, $G = 20$ dB. The P_s/P_0 calculations were made for $f_1 = 25$ MHz ($P_0 = 2$ kW), $f_2 = 45$ MHz ($P_0 = 10$ kw), $f_3 = 100$ MHz ($P_0 = 20$ kW) using the average-daily profiles from Table 1. The calculation results were the following: $P_s/P_0 = -151.9$ dB, -157.7 dB, -154.9 dB, -159.3 dB for f_1; -173.2 dB, -175.5 dB, -167.7 dB, -172.3 dB for f_2; -203.9 dB, -216.5 dB, -204.1 dB, -218.8 dB for f_3. The results given above may be useful for designing radio communication systems.

In order to calculate E-amplitude (field) fluctuations of radio waves, we use the following expression of $\langle I^2 \rangle = \langle \ln(E/E_o)^2 \rangle$ [18]:

$$\langle I^2 \rangle = 0.141 \cdot k^{7/6} \int_0^L C_\varepsilon(r)(L'-r)^{5/6} \, dr, \qquad (3)$$

were E_o is the amplitude of a wave coming into an inhomogeneous medium, $r = z / \sin\alpha_0$, α_0 is the elevation angle, $C_\varepsilon(r) = (80.8 / f^2)^2 D_N$, D_N is the structural function of fluctuations of N, L is distance passed by a wave in the ionosphere.

Calculations were made for the $\langle N(z) \rangle$ profiles from Table 1 and coefficients of the ambipolar diffusion from [1] with a height step of $\Delta z = 2.5$ km. A lower boundary of applicability of the frequency range f_{MUF} was set according to the "cosecant" law: $f_{MUF} = (80.8 < N(z) >^{1/2} \operatorname{cosec}\alpha_0$. Calculation results for the seasons (winter – autumn: a – d, respectively) and $\alpha_0 = 10°$, $20°$, $80°$ (curves 1-3, respectively) are shown in Fig. 1.
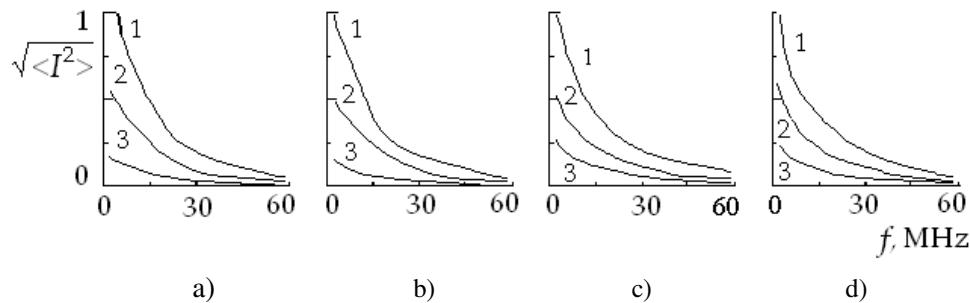

FIG. 1: Model dependences of E-amplitude (field) fluctuations of radio waves for the seasonal average-daily $\langle N(z) \rangle$ profiles (a – d correspond to winter, spring, summer and autumn respectively) and $\alpha_0 = 10^o$, 20°, 80° (curves 1 – 3, respectively)

On the whole, the $\langle I^2 \rangle$ variation depending on the frequency changes considerably over a year at a fixed α_0 value. We found that $f_{MUF} = 5$ MHz for $\alpha_0 = 10°$ and $z = 90$ km.

Phase fluctuations on the radio wave depending on the frequency and the elevation angle of the antenna were calculated using the following expression:

$$\sigma_\phi^2 = \left(\frac{80.8\pi}{c \cdot f} \right)^2 \sum \frac{\int\limits_{\Delta z_i} (\Delta z_i - z)\left(\sigma_N^2 - D_N(z)/2 \right) dz}{\sin^2 \alpha_o - 80.8 < N(\Delta z_i) > / f^2}, \quad (4)$$

were $\Delta z_i = z_i - z_{i-1}$, $i = 1, 2, 3, \ldots, m$; m is the number of radio wave path sections depending on α_0.

The calculation were made for $\alpha_0 = 10°$, $30°$, $80°$ and $f = 5–100$ MHz using the data from Tables 1 and 2. The calculation results are presented in Fig. 2.

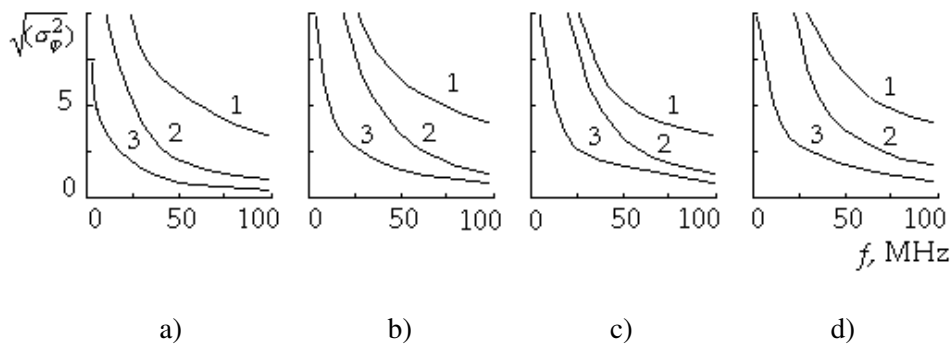a)   b)   c)   d)

FIG. 2: Model dependences of phase fluctuations on the radio waves (a – d correspond to winter, spring, summer and autumn respectively) and $\alpha_0 = 10°$, $30°$, $80°$ (curves 1-3, respectively)

Fluctuations of the angle of arrival α of radio waves depending on f and α_0 were calculated using the following expression from [1]:

$$\langle \alpha_i^2 \rangle = \left(\frac{80.8}{f^2} \right)^2 \frac{L}{4} \int\limits_0^\infty \frac{D_N(r)}{r} dr, \quad (5)$$

Calculations were made for the summer $<N(z)>$ and $d<N>/dz$ profiles (for $\alpha_0 = 10°$, $20°$, $30°$, $80°$ and $f = 5$-100 MHz) using the data from Tables 1 and 2.

The calculation results are presented in Fig. 3 (the curves for $\alpha_0 = 30°$ and $80°$ were practically coincident).

The comparison of the results obtained here with those given in [1] and [19] shows that they coincide in a qualitative manner.

Quantitative differences are determined in the first place by insufficient statistics of the experimental data in [1] and [19]. Besides, high altitudes ($z = 80 – 100$ km) were considered in [1].
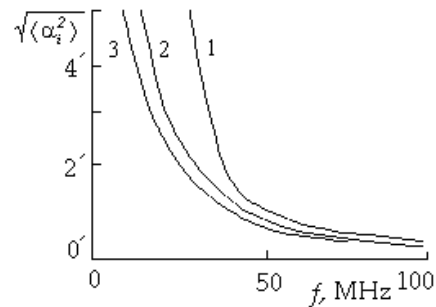
FIG. 3: Model dependences of fluctuations in the angle of arrival of radio waves for summer profiles $\langle N(z) \rangle$ and $d\langle N \rangle/dz$ (for $\alpha_0 = 10°, 20°, 30°$ curves 1 – 3, respectively)

5. CONCLUSIONS

Based on the bank of experimental $N(z)$ profiles obtained in V.N. Karazin Kharkiv National University under non-disturbed conditions by partial reflection technique, there were constructed average-daily seasonal $\langle N(z) \rangle$ and their height gradients $d\langle N \rangle/dz$ profiles. It has been established from the data presented that the main contribution to the total variability of the altitude profiles $N(z)$ in the mid-latitude D-region under non-disturbed conditions is made by meteorological processes and diurnal ionization variability.

Constructed average-daily seasonal $\langle N(z) \rangle$ and their height gradients $d\langle N \rangle/dz$ profiles were used for model calculating characteristics of the radio waves scattered by turbulent N irregularities, which might be useful for designing radio communication system.

REFERENCES

1. Teptin, G.M. and Stenin, Yu.M., (1989) *An Inhomogeneous Structure of the Lower Ionosphere and Propagation of Radio Waves,* Kazan, Russia: Kazan University Publishing House, 97 p., (in Russian).
2. Ginzburg, E.I. and Zhalkovskaya, L.V., (1974) Turbulent effects in the lower ionosphere, *Izvestiya VUZov, Radiofizika,* **14**(4), pp. 301-324, (in Russian).
3. McNamara, L.F., (1979) Statistical model of the D-region, *Radio Sci.*, **14**(6), pp. 1165-1173.
4. Belikovich, V.V., Benediktov, E.A, Vyakhirev, V.D. et al., (1992) The empirical model of the distribution of the electron density of the midlatitude ionospheric D-region, *Geomagnetism and Aeronomy*, **32**(6), pp. 95-103, (in Russian).
5. Smirnova, N.V., Sagidullin, F.S., and Mizun, Yu.G., (1987) *Catalog of the electron concentration profiles in the high-latitude ionosphere obtained by the partial reflection method: comparison with the results of the theoretical model of the D-region*, preprint, Murmansk, Russia: PGI of the USSR Academy of Sciences Publ., **56**, 30 p., (in Russian).
6. Smirnova, N.V., Ogloblin, O.F., and Vlaskov A., (1985) *Models of Electron Concentration in the D-Region of the Ionosphere,* preprint, PGI of the USSR Academy of Sciences Publ., **84-08-36**, 32 p., (in Russian)

7. Nesterova, I.I. and Ginzburg, E.I., (1985) *Catalog of the Electron Concentration Profiles of Region D of the Ionosphere,* Novosibirsk, Russia: IG and G Publ., 210 p., (in Russian).

8. Fatkullin, M.N., Zelenova, T.I., Kozlov, V.K. et al., (1981) *Empirical Models of the Mid-Latitude Ionosphere,* Moscow, Russia: Nauka, 256 p., (in Russian).

9. Friedrich, M. and Torkar, K.M., (1991) D-region electron density model based on rocket borne wave propagation data, *Adv. Space Res.,* **11**(10), pp. 101-104.

10. Danilov, A.D., Rodevich, Yu.A., and Smirnova, N.V., (1991) A parametric model of the D-region, taking account of meteorological effects, *Geomagnetism and Aeronomy*, **31**(5), pp. 881-885, (in Russian).

11. Danilov, A.D. and Ledomskaya, S.Yu. (1983) The empirical model of the region D. Principles of construction and a data bank, *Proceedings of the IEM*, **13**(102), pp. 28-51, (in Russian).

12. Champion, K.S.V., (1990) Middle atmosphere density data and comparison with models, *Adv. Space Res.,* **10**(1), pp. 17-26.

13. Rawer, K., Bossy, L., Kutiev, I. et al., (1990) *International Reference Ionosphere-1990,* Publ., URSI, Committee on Space Research, 58 p.

14. Tyrnov, O.F., Garmash, K.P., Gokov, A.M., Gritchin, A.I. et al., (1994) The Radiophysical Observatory for Remote Sounding of the Ionosphere, *Turkish Journal of Physics*, **18**(11), pp. 1260-1265.

15. Gokov, A.M., Tyrnov, O.F., Buts, Yu.V., and Kovalenko, E.N., (2020) Empirical Modeling of Variations of Electron Density in the Undisturbed Mid-Latitude D-Region of the Ionosphere, *Telecommunications and Radio Engineering*, **79**(4), pp. 335-342.

16. Gokov, A.M., (2014) *Midlatitude Ionospheric D-Region Response to Natural Effects*, Published by: LAP LAMBERT Academic Publishing. Saarbrucken, 300 p. ISBN: 978-3-659-62182-6.

17. Gokov, A.M., (2003) Simultaneous Determination of Electron Density and Electron-Neutral Molecule Collision Frequencies in the Ionospheric D-region by a Partial Reflection Technique, *Telecommunications and Radio Engineering*, **60**(10-12), pp. 145-158.

18. Tatarsky V.I., (1967) *Radio Waves Propagating in the Atmosphere*, Moscow, Russia: Nauka, 548 p., (in Russian).

19. Kolosov M.A., Armand N.A., Yakovleva, S.I., (1969) *Radio Waves Propagating under Radio Communication*, Moscow, Russia: Svyaz, 155 p., (in Russian).